



## Green Synthesis of Silver Nps Based on Arengaengleri Leaves Extract: Characterization and in-Vitrohelicobacter Pylori Activity

Amira B.Mahmoud<sup>1</sup>, Mohamed A. El Reay<sup>2</sup>, Mahmoud Emam<sup>2,3</sup>,

Adel A. H. Abdel-Rahman<sup>1</sup> and Ibrahim F.Zayed<sup>1\*</sup>



CrossMark

<sup>1</sup>Chemistry Department, Faculty of Science, Menoufia University, Egypt

<sup>2</sup>Phytochemistry and Plant Systematics Department, National Research Centre, Dokki, Giza 12622, Egypt

<sup>3</sup>College of Pharmaceutical Science & Collaborative Innovation Center of Yangtze River Delta Region Green Pharmaceuticals, Zhejiang University of Technology, Hangzhou 310014, China

### Abstract

Globally, the infection with *Helicobacter pylori* is considered the most prevalent issue that causes chronic inflammation of the stomach. In this study, the phytochemical investigation of *Arengaengleri* (family Arecaceae) leaves extract that used to prepare the AgNPs was performed and examined for their potential activity against *H. pylori*. The phytochemical results revealed the presence of different phenolic contents depending on the preliminary phytochemical screening, total phenolic content and total flavonoid content measurements, and HPLC profiling. Besides, the percent of unsaturated and saturated fatty acids were 51.39 % and 31.47 %, respectively. The as-prepared AgNPs were characterized by using UV-Vis spectroscopy, IR spectroscopy, TEM, XRD, and Zeta potential. The synthesized AgNPs displayed promising anti *H. pylori* with MIC = 7.81 µg/mL, while the *A. engleri* extract showed weak activity with MIC = 500 µg/mL compared with clarithromycin MIC of 1.95 µg/mL after 3 days of incubation. In conclusion, the organic acids, phenolic, and flavonoid contents of *A. engleri* extract were used as capping agents to prepare simple, low-cost, and effective AgNPs with a particle size range of 10-26 nm that explained their high penetration towards the bacterial cell of *H. pylori* and destroyed it.

**Keywords:** *Arengaengleri*, GC/MS, HPLC, plant extract, Nano particles, phytochemical study.

### 1. Introduction

One of the most dangerous bacterial gastrointestinal infections between adults and children is *Helicobacter pylori*. Besides, to exterminate this infection, multiple antibiotic therapies and a combination of two or three drugs are used. As well, the resistance in bacteria promotes us to find new taps of drugs, and the natural kingdom seems to be an untapped source for promising antibacterial agents [1-3]. In addition, green synthesis of metallic nanoparticles has been adopted to accommodate various bio-materials (e.g., bacteria, fungi, algae, and plant extracts) [4] as a simple and easy process [5] used as antimicrobial agents [6], and possessed antifungal, anti-bacterial, anti-

inflammatory, and anticancer effects [7].

*Arengaengleri* belongs to the family Arecaceae that is previously known as Palmae. This family consists of about 200 genera, contains 2600 species, and widely distributed in tropical and subtropical regions. Also, these palms are famous for the "Trees of Life" nickname due to their potential benefits in humans and animal life [8, 9]. The genus *Arenga* contains twenty-two species that spread in Asia and Australia [10], which are characterized industrially as a source for carbohydrate production and frilly prominence uses [11]. The previous literature recorded the treatment of headaches, malaria, tuberculosis, and skin allergies for different *Arenga* species [12, 13]. They reported hypercholesterolemia,

\*Corresponding author e-mail: [karemshawkey2@gmail.com](mailto:karemshawkey2@gmail.com); (Ibrahim F.Zayed).

EJCHEM use only; Received date 02 September 2021; revised date 17 January 2022; accepted date 06 March 2022

DOI: 10.21608/EJCHEM.2022.93919.4423

©2023 National Information and Documentation Center (NIDOC)

antioxidant, anti-microbial, anti-hypertensive, anti-inflammatory and analgesic activities [14-16]. The reported chemical entities were the chlorophyll a, terpenes, glycerides, flavonoids [17], and phenolics [18].

Arengaengleri, usually known as the Formosa palm, Taiwan sugar palm, or dwarf sugar palm, is a medium-sized decorative clustering palm that is native to Taiwan (Formosa) and Ryukyu Islands (South of Japan). The leaves are known to be useful in thatching and wickerwork. Different phytoconstituents were identified as saturated and unsaturated fatty acids. In addition, saponins, tannins, flavonoids, cardiac glycosides, carbohydrate and/or glycosides, unsaturated sterols, and/or triterpenes were screened to be present while anthraquinones, coumarins, volatiles, and alkaloids were absent [19].

To the best of our knowledge, the in vitro anti-*H. pylori* action of Ag NPs based on the leaves of *A. engleri* was not evaluated before. Therefore, the aims of the recent study were to prepare silver nanoparticles using *A. engleri* leaves extract and investigate the anti-*H. pylori* activity. Additionally, the prepared Ag NPs were characterized using UV, FTIR, TEM, and XRD, phytochemical studies were examined as well.

## 2. Experimental work

### 2.1. Plant material, extraction and Preliminary Qualitative Analysis

Fresh leaves of cultivated *Arengaengleri* were collected from El-Zohria Garden, Cairo, Egypt at March 2020. The leaves of *A. engleri* (100g) powder were extracted by maceration with 1 liter of 70% methanol: water (v:v) mixture at room temperature for 7 days (3 times). The extract was filtered with the filter paper no. 1, the filtrate was collected then concentrated till dryness under reduced pressure (Rotavapor® R-215, BÜCHI, Flawil, Switzerland), and stored at 4°C for further experiments. The extract was screened for its phyto-constituents as flavonoids (Shinoda's test), phenolics (FeCl<sub>3</sub> test), ellagitannins (NaNO<sub>2</sub> assay) and gallotannins (KIO<sub>3</sub> test) [20, 21].

### 2.2. Determination of total phenolic content

The total phenolic content was determined according to the Folin-Ciocalteu procedure [22, 23]. Briefly, the extract (100 µL) was transferred into a test tube and the volume adjusted to 3.5 mL with distilled water and oxidized with the addition of 250

µL of Folin-Ciocalteu reagent. After 5 min, the mixture was neutralized with 1.25 mL of 20% aqueous sodium carbonate (Na<sub>2</sub>CO<sub>3</sub>) solution. After 40 min, the absorbance was measured at 725 nm against the solvent blank. The total phenolic content was determined by means of a calibration curve prepared with gallic acid, and expressed as µg of gallic acid equivalent (mg GAE) per g of sample.

### 2.3. Determination of total flavonoid content

The total flavonoid content was determined according to Zilicet al. (2012) using aluminum chloride (AlCl<sub>3</sub>) colorimetric assay. Briefly, 300 µL of 5% sodium nitrite (NaNO<sub>2</sub>) was mixed with 100 µL of extract. After 6 min, 300 µL of a 10% AlCl<sub>3</sub> solution was added and the volume was adjusted to 2.5 mL using distilled water. After 7 min, 1.5 mL of 1 M NaOH was added, and the mixture was centrifuged at 5000 g for 10 min. Absorbance of the supernatant was measured at 510 nm against the solvent blank. The total flavonoid content was determined by means of a calibration curve prepared with catechine, and expressed as milligrams of catechin equivalent (mg CE) per g of sample. Additional dilution was done if the absorbance value measured was over the linear range of the standard curve.

### 2.4. Gas chromatography–mass spectrometry analysis (GC-MS)

The GC-MS system (Agilent Technologies) was equipped with gas chromatograph (7890B) and mass spectrometer detector (5977A) at Central Laboratories Network, National Research Centre, Cairo, Egypt. The GC was equipped with HP-5MS column (30 m x 0.25 mm internal diameter and 0.25 µm film thickness). Analyses were carried out using Hydrogen as the carrier gas at a flow rate of 1.0 ml/min at a splitless, injection volume of 1 µl and the following temperature program: 50 °C for 1 min; rising at 10 °C /min to 300 °C and held for 20 min. The injector and detector were held at 250 °C. Mass spectra were obtained by electron ionization (EI) at 70 eV; using a spectral range of m/z 30-700 and solvent delay 9 min. The mass temperature was 230°C and Quad 150 °C. Identification of different constituents was determined by comparing the spectrum fragmentation pattern with those stored in Wiley and NIST Mass Spectral Library data.

### 2.5. HPLC conditions

HPLC analysis was carried out using an

Agilent 1260 series. The separation was carried out using Eclipse C18 column (4.6 mm x 250 mm i.d., 5  $\mu$ m). The mobile phase consisted of water (A) and 0.05% trifluoroacetic acid in acetonitrile (B) at a flow rate 1 ml/min. The mobile phase was programmed consecutively in a linear gradient as follows: 0 min (82% A); 0–5 min (80% A); 5–8 min (60% A); 8–12 min (60% A); 12–15 min (85% A) and 15–16 min (82% A). The multi-wavelength detector was monitored at 280 nm. The injection volume was 10  $\mu$ l for each of the sample solutions. The column temperature was maintained at 35 °C.

### 2.6. Preparation of Nano silver (AgNPs)

Serial concentration of Dissolved plant extract (40mg/10 ml of DMSO) were react with 10 ml of (1Mm) of silver nitrate solution then the mixture kept in magnetic stirrer/orbital shaker and left for one day in dark for nanoparticle synthesis. The colour change was observed visually and photographs were recorded.

The nanoparticles solution if centrifuged using to lark refrigerated centrifuge. The solution of the nanoparticles is centrifuged at 8000rpm for 10 minutes and the pellet is collected and washed with distilled water twice. The final purified pellet is collected and dried at 60 degree Celsius for 2-4 hours. Finally, the nanoparticles powder is collected and stored in air tight tube [24].

### 2.7. Characterisation of nanoparticles

The synthesized nanoparticles solution is preliminary characterized by using UV-VIS-Spectroscopy. 3ml of the solution is taken in cuvette and scanned in double beam UV-VIS-Spectrophotometer from 300nm to 700nm wavelength. The results were recorded for the graphical analysis. The crystalline structure of NPs were characterized by X-ray diffraction (XRD) using a Philips PW 1840 diffractometer (Mahwah, NJ, USA). CuK $\alpha$  radiation of 1.5406Å wavelength at 40 kV and 30 mA was used to expose the samples through a Ni filter. The 2 $\theta$  values were set in the range of 10°–65°. Peaks on the X-ray patterns recorded for the sample were compared with standard XRD pattern of NPs (Joint Committee on Powder Diffraction Standards [JCPDS] card No 13-0311). The mean crystallite size was calculated using the Scherer equation. Fourier transformed infrared (FT-IR) spectrum was obtained with Perkin-Elmer-1430 (Perkin Elmer, Waltham, MA, USA) using KBr pellet

technique for the range 4.000 and 400 cm<sup>-1</sup>. The nanostructures and size distribution of the synthetic particles were examined by transmission electron microscopy (TEM) using a JEM 100SX (JEOL, Co., Akishima, Japan) operating at an acceleration voltage of 80 kV. The specimens for TEM investigations were prepared by placing a drop of NPs suspension on a carbon-coated copper grid (400 mesh)

### 2.8. Anti -Helicobacter pylori Activity

Antibacterial activity of tested compounds against *H. pylori* ATCC 700392, was determined by a micro-well dilution method. The inoculum of *Helicobacter pylori* was prepared and the suspensions were adjusted to 10<sup>6</sup> CFU/ml. The compounds under investigation and the standard drug (Clarithromycin) were prepared in dimethyl sulfoxide (DMSO) and subsequent twofold dilutions (1000- 0.03  $\mu$ g) were performed in a 96-well plate. Each well of the microplate included 40  $\mu$ l of the growth medium (Brain Heart Infusion (BHI) plus 10% fetal bovine serum (FBS), 10  $\mu$ l of inoculum and 50  $\mu$ l of the diluted compounds. The Clarithromycin and DMSO are used as positive and negative controls, respectively. The plates were incubated at 37°C for 3 days, in 5% O<sub>2</sub>, 10% CO<sub>2</sub>, 85% N<sub>2</sub> atmosphere. After that, 40  $\mu$ l of 3- (4, 5-dimethyl-thiazol-2-yl)- 2,5-diphenyl-tetrazolium bromide (MTT) at a final concentration 0.5 mg/ml freshly prepared in water was added to each well and incubated for 30 min. The change to purple colour indicated that the bacteria were biologically active. The inhibition percentage was calculated using the given formula:

$$\% \text{inhibition} = \frac{\text{Abs Control} - \text{Abs Sample}}{\text{Abs Control}} \times 100$$

The concentration of samples (inhibitors) required for 90% of inhibition (MIC 90) was determined from corresponding dose-response curves. The MIC was taken to the lowest concentration, where no change of colour of MTT was determined using an automatic ELISA microplate reader at 620 nm. The MIC values were done in triplicate.

## 3. Results and discussion

### 3.1. Phytochemical studies

#### 3.1.1. Preliminary phenolic phytochemicals screening

The preliminary phytochemical screening of *A. engleri* extract exhibited dark green color after adding the ferric chloride solution that revealed the presence

of phenolics. In addition the light red color of Shinoda's test revealed to the light presence of flavonoids and/or their glycosides. While, the gallotannins and ellagitannins moieties were absent after adding potassium iodate ( $\text{KIO}_3$ ) and sodium nitrite ( $\text{NaNO}_2$ ), respectively.

**Table 1**

Phenolic constituents of the <i>A. engleri</i> extract	
Test	Observation
Ferric chloride $\text{FeCl}_3$ (1%) Shinoda's (Mg/conc. HCl)	Dark green (+ve) Light red (+ve)
Potassium Iodate ( $\text{KIO}_3$ )	-Ve
Sodium nitrite ( $\text{NaNO}_2$ )	-Ve

+ve: positive, -ve: negative

### 3.1.2. Total phenolic (TPC) and flavonoid (TFC) contents

The TPC and TFC of *A. engleri* extract were estimated by using gallic acid and catechin as standards, respectively. Both standard concentrations were conformed to Beer's Law at 725 nm and 510 nm, respectively to determine the regression coefficient ( $R^2$ ), slope (m) and the intercept for each standard curve equation (Figure 1 and Figure 2). Consequently, the TPC and TFC of *A. engleri* extract were estimated as 41.03 GAE/g and 25.6 CE/g, respectively.

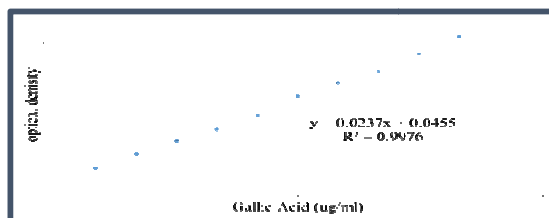


**Fig. 1:** Total phenolic content for standard gallic acid

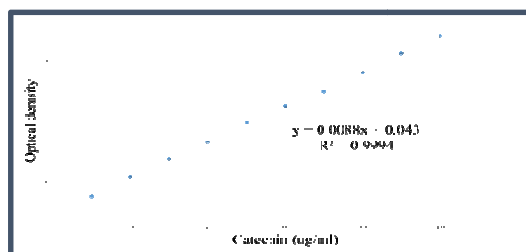


**Fig. 2:** Total flavonoid content for standard Catechin

### 3.1.3. HPLC analysis of *A. engleri* extract

The HPLC analysis of *A. engleri* extract was shown in Table 2. The HPLC analysis reveals that the liquid extract of *A. engleri* contain Multi reducing agents like protocatechuic acid, chlorogenic acid, catechin, caffeic acid and p-coumaric acid which provide the powerful reduction for silver  $^{+1}$ .

**Table 2**

HPLC analysis of *A. engleri* leaves extract

No	Rt (min)	Constituents	Conc(mg/g)
1	3.11	Protocatechuic acid	11045.15
2	3.78	Chlorogenic acid	1097.42
3	4.23	Catechin	302.37
4	5.56	Caffeic acid	1996.66
5	5.98	Syringic acid	1481.41
6	6.65	Pyrocatechol	0.00
7	7.32	Rutin	5748.54
8	7.95	Isorhamnetin-3-o-rutinoside	9599.57
9	8.15	Coumaric acid	1604.09
10	8.94	Vanillin	65.82
11	9.66	Ferulic acid	2338.68
12	9.91	Naringenin	1823.67
13	11.99	Taxifolin	148.15
14	13.32	Cinnamic acid	62.15
15	14.04	Kaempferol	134.91

### 3.1.4. Investigation of extract of *A. engleri* leaves using GCMS

Fractionation of *A. engleri* plant extract was shown in Table 3, GC-MS results of unsaponifiable matter revealed that *A. engleri* extract contain 33.21% different hydrocarbons, 25.63% fatty alcohols, 5.65% terpenes and 2% sterols. The most abundant compounds identified in hydrocarbons content were 1-octadecene (15.21%) and 1-hexadecene (8.32%). Total terpenes identified as 4.89% phytol and 4.79% squalene.

## 3.2. Characterization of Nano silver (AgNPs)

### 3.2.1. UV-Vis Spectroscopic Studies

UV visible Spectroscopic Study: the process of the bio-reduction of  $\text{Ag}^+$  ions using extract of *A. engleri* as reducing agent and stabilizing agent, monitored from the increasing intensity of surface plasmon resonance/ absorption peak of silver nanoparticles around 430 nm. Surface plasmon resonance (SPR) absorption patterns, of metal nanoparticles, depends on particle size and the dielectric constant of the medium. SPR bands observed, with increase in the reaction time indicates the formation of anisotropic molecules that are stabilized in the medium. Absorption of visible radiation is due to the induced polarization in conduction electrons of metal

nanoparticles with respect to their immobile nucleus. When a particular wavelength is matched to the size of nanoparticle, dipole oscillation is generated in the compensated form of the induce polarization and then

the electrons in the nanoparticle resonate, resulting in absorption of radiation. The peak at 430 nm for silver nano particles is due to the excitation of longitudinal Plasmon vibrations [25].

**Table 3**  
GC-MS analysis of *A. engleri* leaves extract

Peak	RT	RTT	Name	Class	Formula	Area Sum %
	17.534	0.89	10-Methyl-E-11-tridecen-1-ol propionate	Fatty Ester	C <sub>17</sub> H <sub>32</sub> O <sub>2</sub>	2.13
	17.64	0.90	Myristic acid, TMS derivative	Fatty acid	C <sub>17</sub> H <sub>36</sub> O <sub>2</sub> Si	3.81
	17.971	0.92	8,11,14-Eicosatrienoic acid, (Z,Z,Z)-	Fatty Acid	C <sub>20</sub> H <sub>34</sub> O <sub>2</sub>	1.72
	19.35	0.99	1,12-Tridecadiene	Hydrocarbon	C <sub>13</sub> H <sub>24</sub>	2.58
	19.524	1	Palmitic Acid, TMS derivative	Fatty Acid	C <sub>19</sub> H <sub>40</sub> O <sub>2</sub> Si	12.76
	20.217	1.03	5,8,11,14-Eicosatetraenoic acid, methyl ester, (all-Z)-	Fatty Acid	C <sub>21</sub> H <sub>34</sub> O <sub>2</sub>	9.84
	20.609	1.05	9-Octadecenoic acid (Z)-	Fatty Acid	C <sub>18</sub> H <sub>34</sub> O <sub>2</sub>	3.54
	20.692	1.06	17-Octadecynoic acid	Fatty Acid	C <sub>18</sub> H <sub>32</sub> O <sub>2</sub>	5.77
	21.046	1.07	13-Heptadecyn-1-ol	Sterol	C <sub>17</sub> H <sub>32</sub> O	1.06
	21.732	1.11	9-Octadecenal	Hydrocarbon	C <sub>18</sub> H <sub>34</sub> O	3.72
	23.171	1.18	7,11-Hexadecadienal	Hydrocarbon	C <sub>16</sub> H <sub>28</sub> O	10.36
	23.344	1.19	1,2-15,16-Diepoxyhexadecane	Hydrocarbon	C <sub>16</sub> H <sub>30</sub> O <sub>2</sub>	2.22
	25.251	1.29	9,12,15-Octadecatrienoic acid, 2,3-dihydroxypropyl ester, (Z,Z,Z)-	Fatty acid	C <sub>21</sub> H <sub>36</sub> O <sub>4</sub>	3.84
	25.409	1.30	8,11,14-Eicosatrienoic acid, methyl ester, (Z,Z,Z)-	Fatty Acid	C <sub>21</sub> H <sub>36</sub> O <sub>2</sub>	0.49
	26.69	1.36	6,9,12,15-Docosatetraenoic acid, methyl ester	Fatty Acid	C <sub>23</sub> H <sub>38</sub> O <sub>2</sub>	1.91
	27.044	1.38	Hi-oleic safflower oil	Sterol	C <sub>21</sub> H <sub>22</sub> O <sub>11</sub>	0.94
	28.302	1.44	9-Octadecen-12-ynoic acid, methyl ester	Fatty acid	C <sub>19</sub> H <sub>32</sub> O <sub>2</sub>	3.74
	29.651	1.51	Z,Z-3,15-Octadecadien-1-ol acetate	Sterol	C <sub>20</sub> H <sub>36</sub> O <sub>2</sub>	0.59
	31.882	1.63	Stigmasta-5,22-dien-3-ol, acetate, (3β)-	Sterol	C <sub>31</sub> H <sub>50</sub> O <sub>2</sub>	1.12
	35.521	1.81	5.beta.,7.beta.H,10.alpha.-Eudesm-11-en-1.alpha.-ol	Sterol	C <sub>15</sub> H <sub>26</sub> O	6.03
	35.921	1.84	Z,Z,Z-4,6,9-Nonadecatriene	Hydrocarbon	C <sub>19</sub> H <sub>34</sub>	2.11

RRT\*: Relative retention time of Palmitic acid with RT = 19.524 min.

### 3.2.2. FTIR Spectroscopic Studies

The phytochemical results show that the leaves extract of *A. engleri* consisting of a complex mixture of phytochemicals such as hydrocarbones, fatty Acids, flavonoids, plant sterols, carbohydrates or glycosides. These phytochemical species are rich in hydroxyl and amino groups. Several reports attributed the reduction of the metal nanoparticles to the presence of such functional groups. Hence, the FTIR is a sensitive tool for determining the

functional groups responsible for the Ag nanoparticles reduction. Figure 4 showed the FTIR spectra of the *A. engleri-stabilized Ag* nanoparticles.

### 3.1.3. TEM Studies

The shape and size of the prepared Ag NPs are assessed using the HRTEM technique. Figure 5 shows the TEM image of the prepared Ag NPs that can be seen mainly spherical in shape with particle size varies between 10-49 nm. The particles are

separated from each other which reflect the capping action of the plant extract in the preparation process. The results indicate that synthetic Ag NPs have well-dispersed Ag NPs.

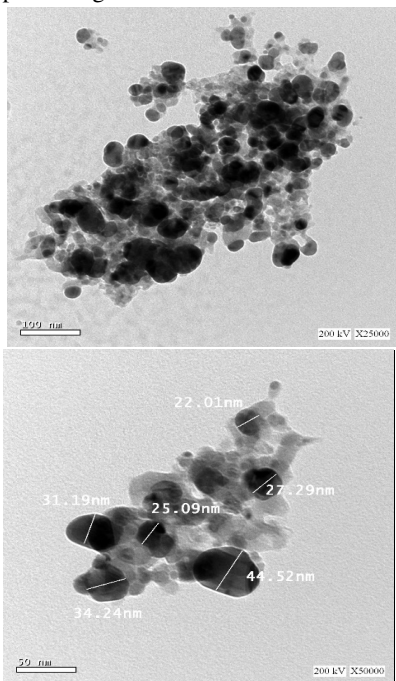


**Figure 5.** The TEM images of *A. engleri*-stabilized Ag nanoparticles

### 3.2.4. XRD studies

The crystalline nature, phase variety, and grain size of synthesized silver nanoparticles were determined by X-ray diffraction spectroscopy. The particle size of the prepared samples was determined by using Scherrer's equation as follows:

$$D = K\lambda / (\beta \cos \theta)$$

Where D is average crystallite size and  $\beta$  is line broadening in radians (full width at half maximum of the peak in radians).  $\lambda$  is wavelength of X-ray and  $\theta$  is bragg angle. K is constant (geometric factor = 0.94). The XRD analysis of synthesized silver nanoparticles from *A. engleri* extract showed diffraction peaks at  $2\theta = 27.5^\circ, 32.2^\circ, 46.4^\circ, 55^\circ, 57.2^\circ$  and  $77^\circ$ . When compared with the standard, the obtained XRD spectrum confirmed that the synthesized silver nanoparticles were in nanocrystal form and crystalline in nature. The peaks can be assigned to the planes (122), (111), (200), (220), and (311) facet of silver crystal, respectively. The high peaks in the XRD analysis indicated the active silver composition with the indexing. Figure 6 shows XRD pattern of the synthetic AgNPs produced by co-

precipitation method.

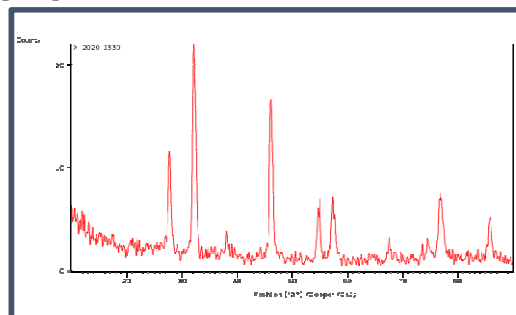


**Figure 6.** XRD pattern of AgNPs

### 3.3. Biological activity

Silver nanoparticles prepared by the process in our study, are quite fast and low cost. *H. pylori* infection is the most common cause of chronic inflammation of the stomach worldwide. The bacterium discovered by Warren and Marshall in 1982 colonizes around half of the world population. All *H. pylori* infected individuals could develop chronic gastritis. *H. pylori* have a high global prevalence, especially in developing countries [26-28]. Despite the high prevalence of *H. pylori* infection, it is estimated that 1% of infected people will develop noncardia gastric cancer. Though the oral administration of antibacterial agents, such as amoxicillin, Clarithromycin and metronidazole, is carried out around the world to treat patients infected with *H. pylori*, resistance against these antibacterial agents has been increasing year after year [29, 30]. As a result a great need has arisen to discover and develop new anti-*H. pylori* remedies especially from herbs that not only will eradicate and possibly prevent the organism, but also would have minimal side effects, be easily accessible, and be affordable even for the poor. *Helicobacter pylori*, a Gram-negative microaerophilic bacterium that colonizes the human gastric mucosa is thought to infect half the world population. In infected individuals, *H. pylori* causes chronic gastric inflammation, which progresses in a significant fraction of cases to peptic ulcer, MALT-lymphoma, or gastric adenocarcinoma, the latter being a major cause of cancer-related deaths worldwide. Accordingly, the bacterium was classified as a class I carcinogen by the International Agency for Research on Cancer in 1994. More recently, the results of 12 studies including 1228 cancer cases and 3406 controls showed that *H. pylori*-positive individuals have at least a 6-fold increased risk of

developing gastric cancer than *H. pylori*-negative individuals [31].

**Table 3**  
Anti-*Helicobacter pylori* activity

Samples	Minimum Inhibitory concentration (MIC) ( $\mu\text{g/ml}$ )
AE	500
AgNPs	7.81
Clarithromycin	1.95

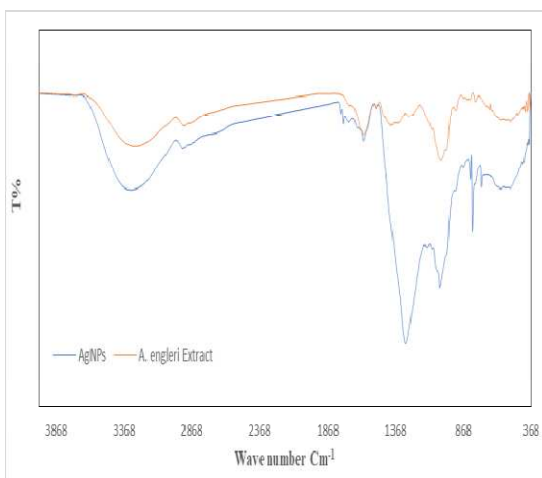


**Figure 4.** FTIR spectra of extract stabilized Ag nanoparticles

#### 4. Conflicts of interest

There are no conflicts of interest to declare.

#### 5. Acknowledgments

This work was supported by the National Research Centre, Egypt [Project Number 12010123]. Also, we wish to thank the Regional Center for Mycology and Biotechnology, Al-Azhar University, Cairo, Egypt for *Helicobacter pylori* studies.

#### 6. References

1. Marshall BJ, Warren JR. Unidentified curved bacilli in the stomach of patients with gastritis and peptic ulceration. *Lancet*. 1984;1:1311–1315.
2. Kandulski A, Selgrad M, Malfertheiner P. *Helicobacter pylori* infection: a clinical overview. *Dig Liver Dis*. 2008;40:619–626.
3. McColl KE. Clinical practice. *Helicobacter pylori* infection. *N Engl J Med*. 2010;362:1597–1604.
4. Lopes D, Nunes C, Martins MC, Sarmiento B, Reis S. Eradication of *Helicobacter pylori*: Past,

present and future. *J Control Release*. 2014;189:169–186.

5. Wang Y, Wang B, Lv ZF, Yang Y, Wang F, Wang H, Chen S, Xie Y, Zhou X. Efficacy and safety of ecabet sodium as an adjuvant therapy for *Helicobacter pylori* eradication: a systematic review and meta-analysis. *Helicobacter*. 2014;19:372–381.
6. NIH Consensus Conference. *Helicobacter pylori* in peptic ulcer disease. NIH Consensus Development Panel on *Helicobacter pylori* in Peptic Ulcer Disease. *JAMA*. 1994;272:65–69.
7. Bytzer P, Dahlerup JF, Eriksen JR, Jarbøl DE, Rosenstock S, Wildt S. Diagnosis and treatment of *Helicobacter pylori* infection. *Dan Med Bull*. 2011;58:C4271.
8. Tytgat GN. Etiopathogenetic principles and peptic ulcer disease classification. *Dig Dis*. 2011;29:454–458.
9. Testerman TL, Morris J. Beyond the stomach: an updated view of *Helicobacter pylori* pathogenesis, diagnosis, and treatment. *World J Gastroenterol*. 2014;20:12781–12808.
10. Georgopoulos SD, Papastergiou V, Karatapanis S. Current options for the treatment of *Helicobacter pylori*. *Expert Opin Pharmacother*. 2013;14:211–223.
11. Freeman HJ. Disappearance of *Helicobacter* without antibiotics in 12 patients with gastritis. *Can J Gastroenterol*. 1997;11:167–172.
12. Go MF. Review article: natural history and epidemiology of *Helicobacter pylori* infection. *Aliment Pharmacol Ther*. 2002;16Suppl 1:3–15.
13. Fakheri H, Bari Z, Aarabi M, Malekzadeh R. *Helicobacter pylori* eradication in West Asia: a review. *World J Gastroenterol*. 2014;20:10355–10367.
14. Bouvard V, Baan R, Straif K, Grosse Y, Secretan B, El Ghissassi F, Benbrahim-Tallaa L, Guha N, Freeman C, Galichet L, et al. A review of human carcinogens--Part B: biological agents. *Lancet Oncol*. 2009;10:321–322.
15. Fukase K, Kato M, Kikuchi S, Inoue K, Uemura N, Okamoto S, Terao S, Amagai K, Hayashi S, Asaka M. Effect of eradication of *Helicobacter pylori* on incidence of metachronous gastric carcinoma after endoscopic resection of early gastric cancer: an open-label, randomised controlled trial. *Lancet*. 2008;372:392–397.
16. Suzuki H, Nishizawa T, Hibi T. *Helicobacter pylori* eradication therapy. *Future Microbiol*. 2010;5:639–648.
17. Nishizawa T, Nishizawa Y, Yahagi N, Kanai T, Takahashi M, Suzuki H. Effect of supplementation with rebamipide for *Helicobacter pylori* eradication therapy: a

- systematic review and meta-analysis. *J GastroenterolHepatol.* 2014;29Suppl 4:20–24.
18. Molina-Infante J, Gisbert JP. Optimizing clarithromycin-containing therapy for *Helicobacter pylori* in the era of antibiotic resistance. *World J Gastroenterol.* 2014;20:10338–10347.
  19. Gisbert JP, González L, Calvet X, García N, López T, Roqué M, Gabriel R, Pajares JM. Proton pump inhibitor, clarithromycin and either amoxicillin or nitroimidazole: a meta-analysis of eradication of *Helicobacter pylori*. *Aliment PharmacolTher.* 2000;14:1319–1328.
  20. El-mekawy, S.; Shahat, A.A.; Alqahtani, A.S.; Alsaid, M.S.; Abdelfattah, M.A.; Ullah, R.; Emam, M.; Yasri, A.; Sobeh, M. A Polyphenols-Rich Extract from *Moricandiasinaica* Boiss. Exhibits Analgesic, Anti-Inflammatory and Antipyretic Activities In Vivo. *Molecules* 2020, 25, 5049.
  21. El-Garawani, I.; Emam, M.; Elkhateeb, W.; El-Seedi, H.; Khalifa, S.; Oshiba, S.; Abou-Ghanima, S.; Daba, G. In Vitro Antigenotoxic, Antihelminthic and Antioxidant Potentials Based on the Extracted Metabolites from Lichen, *Candelariellavitellina*. *Pharmaceutics* 2020, 12, 477.
  22. S.M. Mandal, D. Chakraborty, S. Dey Phenolic acids act as signaling molecules in plant-microbe symbioses *Plant Signal Behav*, 5 (4) (2010), pp. 359-368
  23. K.B. Pandey, S.I. Rizvi Plant polyphenols as dietary antioxidants in human health and disease *Oxid Med Cell Longev*, 2 (5) (2009), pp. 270-278
  24. Sujatha J, Asokan S, Rajeshkumar S. Antidermatophytic activity of green synthesised zinc oxide nanoparticles using *Cassia alata* leaves. *J MicrobiolBiotechnol Food Sci* 2018;7:348-52.
  25. SoumyaMenon, Shrudhi Devi KS, Santhiya R, Rajesh kumar S, Venkat Kumar S, Selenium nanoparticles: A potent chemotherapeutic agent and an elucidation of its mechanism, *Colloids and Surfaces B: Biointerfaces*
  26. Malaty, H. M., and D. Y. Graham. 1994. Importance of childhood socioeconomic status on the current prevalence of *Helicobacter pylori* infection. *Gut* 35:742-745.
  27. Morris, A., and G. Nicholson. 1987. Ingestion of *Campylobacter pyloridis* causes gastritis and raised fasting gastric pH. *Am. J. Gastroenterol.* 82:192-199.
  28. Morris, A. J., M. R. Ali, G. I. Nicholson, G. I. Perez-Perez, and M. J. Blaser. 1991. Long-term follow-up of voluntary ingestion of *Helicobacter pylori*. *Ann. Intern. Med.* 114:662-663.
  29. Bytzer P, Dahlerup JF, Eriksen JR, Jarbøl DE, Rosenstock S, Wildt S. Diagnosis and treatment of *Helicobacter pylori* infection. *Dan Med Bull.* 2011;58:C4271.
  30. Testerman TL, Morris J. Beyond the stomach: an updated view of *Helicobacter pylori* pathogenesis, diagnosis, and treatment. *World J Gastroenterol.* 2014;20:12781–12808.
  31. Freeman HJ. Disappearance of *Helicobacter* without antibiotics in 12 patients with gastritis. *Can J Gastroenterol.* 1997;11:167–172.